

Percolation transitions in pyrochlore: Radiation-damage and thermally induced structural reorganization

Cite as: Appl. Phys. Lett. **119**, 131905 (2021); <https://doi.org/10.1063/5.0068685>

Submitted: 26 August 2021 • Accepted: 13 September 2021 • Published Online: 28 September 2021

 Tobias Beirau and  Norbert Huber



View Online



Export Citation



CrossMark

ARTICLES YOU MAY BE INTERESTED IN

[Hetero-deformation-induced \(HDI\) plasticity induces simultaneous increase in both yield strength and ductility in a \$\text{Fe}_{50}\text{Mn}_{30}\text{Co}_{10}\text{Cr}_{10}\$ high-entropy alloy](#)

Applied Physics Letters **119**, 131906 (2021); <https://doi.org/10.1063/5.0065148>

[High thermoelectric power factors in polycrystalline germanium thin films](#)

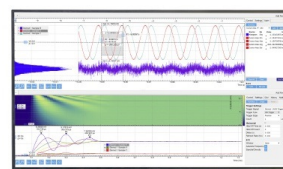
Applied Physics Letters **119**, 132101 (2021); <https://doi.org/10.1063/5.0056470>

[Effect of short-range order on the mechanical behaviors of tensile and shear for NiCoFeCr](#)

Applied Physics Letters **119**, 131904 (2021); <https://doi.org/10.1063/5.0064420>

Challenge us.

What are your needs for periodic signal detection?



Zurich Instruments

Percolation transitions in pyrochlore: Radiation-damage and thermally induced structural reorganization

Cite as: Appl. Phys. Lett. **119**, 131905 (2021); doi: [10.1063/5.0068685](https://doi.org/10.1063/5.0068685)

Submitted: 26 August 2021 · Accepted: 13 September 2021 ·

Published Online: 28 September 2021



View Online



Export Citation



CrossMark

Tobias Beirau^{1,a)}  and Norbert Huber^{2,3,a)} 

AFFILIATIONS

¹Institute of Geosciences and Geography, Mineralogy/Geochemistry, Martin Luther University Halle-Wittenberg, 06120 Halle, Germany

²Institute of Materials Mechanics, Helmholtz-Zentrum Hereon, 21502 Geesthacht, Germany

³Institute of Materials Physics and Technology, Hamburg University of Technology (TUHH), 21073 Hamburg, Germany

^{a)}Authors to whom correspondence should be addressed: tobias.beirau@geo.uni-halle.de and norbert.huber@hereon.de

ABSTRACT

Finite element mechanical modeling is used to follow the evolution of the hardness (H), Young's modulus (E), and Poisson's ratio (ν) during the radiation-damage related crystalline-to-amorphous transition in pyrochlore (average main composition $\text{Ca}_2\text{Nb}_2\text{O}_6\text{F}$). According to the model, two percolation transitions have been identified around 16% and 84% amorphous volume fraction, respectively. In this context, earlier results from thermally induced recrystallization experiments have found to indicate noticeable modifications on the short- and long-range order by passing the percolation thresholds. Both percolation points have found to act as specific kinetic barriers during stepwise annealing induced structural reorganization. As phases with pyrochlore structure have been considered as host structures for the long-term disposal of actinides, it is essential to gain better knowledge of their mechanical behavior under radiation-damage and subsequent temperature treatment. The obtained results validate the used models' robustness in predicting radiation-damage related mechanical modifications, at least for ceramics.

© 2021 Author(s). All article content, except where otherwise noted, is licensed under a Creative Commons Attribution (CC BY) license (<http://creativecommons.org/licenses/by/4.0/>). <https://doi.org/10.1063/5.0068685>

Materials with pyrochlore structure ($\text{A}_2\text{B}_2\text{O}_7$) hold a wide range of technically important properties, e.g., giant magnetoresistance, catalytic abilities, luminescence, ferromagnetism, and piezoelectricity,^{1–5} and have been considered as host phases for long-term nuclear waste disposal.^{2,6,7} Pyrochlore (ideal formula $\text{A}_2\text{B}_2\text{X}_6\text{Y}$) crystallizes in the cubic space group $Fd\bar{3}m$ with eightfold coordinated A cations building A_2Y chains and corner-sharing BX_6 octahedra.⁸ The mineral can incorporate a large variety of different cations on the A and B positions. This includes rare earth and radioactive elements, as up to 9 wt. % ThO_2 and 30 wt. % UO_2 have been reported.⁹ The oxygen on the X and Y positions can be replaced by OH and fluorine on the latter (for details, see Ref. 10). The incorporated actinides lead, mainly by α -decay, to structural damage in the initially periodic structure (see Ref. 11). During this process, two kinds of particles are created: the α -particle (helium core) and a heavy recoil nucleus. While the α -particle loses most of its energy by electronic extinctions and causes only several hundred atom displacements, most at the end of its path,

the heavy recoil nucleus displaces several thousand atoms on its path by elastic collisions. The so (by the latter) induced recoil cascades overlap with increasing structural damage, leading to an extremely disordered (so-called metamict) state.

The radiation-damaged state is metastable, while thermal annealing leads (at least partially) to structural reorganization.^{12–14} Nevertheless, this process has found to be not a simple reverse process of the initial damage event in, e.g., zircon and titanite.¹⁵ During the thermally induced recrystallization of heavily damaged pyrochlore, avalanches have been detected, as phase fronts move by local singularities.¹⁶ Furthermore, a statistically similarity to the switching of ferroelectrics and the collapse of martensites induced by external pressure has been reported.¹⁶

The radiation damage induced crystalline-to-amorphous transition, at least in zircon, can be described in terms of percolation theory,¹⁷ which has also been suggested for pyrochlore.¹⁸ Up to the first percolation point, only the crystalline fraction percolates. After passing

this threshold, both crystalline and amorphous fractions percolate, while by reaching the second percolation point, the crystalline fraction ceases to percolate. A mechanical modeling approach that uses finite element-voxel models to determine the macroscopic elastic properties of bi-continuous microstructures (crystalline and amorphous phases in the present case) with two percolation points¹⁹ has recently found to be sufficient to simulate the crystalline-to-amorphous transition in zircon (for details, see Ref. 20). It is based on structural topology, generated by level-cut random Gaussian fields,^{21,22} and predicts two volumetric percolation thresholds at $\phi_a^{P1} = 15.9\%$ and $\phi_a^{P2} = 84.1\%$.¹⁹ Elastic-plastic finite element simulations of the representative volume element (RVE) allow to compute the density, Young's modulus, Poisson's ratio, yield stress, hardness, and volumetric swelling as a function of amorphous phase fraction (f_a).²⁰

In this Letter, we employ the modeling approach by Ref. 20 together with experimental nanoindentation data¹⁴ to clarify: (i) if the radiation induced crystalline-to-amorphous transition in pyrochlore can be adequately described as a percolation problem with two percolation points and if so, (ii) do the percolation thresholds affect the thermally induced structural reorganization?

Although the used model describes an isotropic case, reference data used for calibration were obtained from three macroscopic (111) oriented pyrochlore samples, with different degrees of structural disorder and the average main composition $\text{Ca}_2\text{Nb}_2\text{O}_6\text{F}$.¹³ As initial input parameters for the simulation an E of 235 GPa and an H of 12.5 GPa have been chosen for the crystalline phase, the E is an average value obtained from ceramics with pyrochlore structure of the composition $(\text{Ca}_2\text{Nb}_2\text{O}_7)_{0.25-0.5}(\text{Gd}_2\text{Zr}_2\text{O}_7)_{0.5-0.75}$,²³ and the H value is an initial assumption, based on the literature value for recrystallized initially less damaged Panda Hill pyrochlore [$H \sim 12.2$ GPa (Ref. 14)]. While an E value of 110 GPa and an H value of 7.55 GPa have been taken for the amorphous phase in close approximation to the highly damaged Miass pyrochlore sample (100% f_a after Ref. 13), the elastic constants of both phases have been adjusted by fitting the predicted macroscopic response of the RVE to the measured behavior of the Young's modulus¹⁴ as a function of the average calculated amorphous fraction¹³ of reference pyrochlores before and after annealing (Fig. 1). An initial Poisson's ratio (ν) of 0.27 has been used that fits very well into the range reported for rare earth stannate pyrochlores.²⁴ As the amorphization causes volume expansion, a volumetric swelling of $\sim 5.4\%$ is achieved in this study that is in good agreement with literature data of $\sim 5\%$ – 6% reported for synthetic Cm or Pu doped pyrochlore (structure) and zirconolite.^{2,25,26}

Figure 1 shows the modeled evolution of the macroscopic mechanical properties Young's modulus (E), Poisson's ratio (ν), and hardness (H) with increasing amorphization. Both volumetric percolation thresholds (p_{c1} and p_{c2}) at 15.9% and 84.1% f_a , respectively, are model dependent and have been determined previously by Soyarslan *et al.*,¹⁹ consistent with the points where the Gaussian curvature of the surface of the specific phase volume fraction as well as the scaled genus density equals zero. In contrast to Ref. 20, a good fit is obtained with a simplified model without an interface, resulting in a nearly linear trend for the hardness. The Poisson's ratio stays relatively constant between ~ 0.265 and 0.27 , with the minimum at 50% f_a . The used approach assumes an inverse relationship between the crystalline-to-amorphous transition and the thermally induced reverse process. This seems in the case of pyrochlore under the given conditions a reasonable

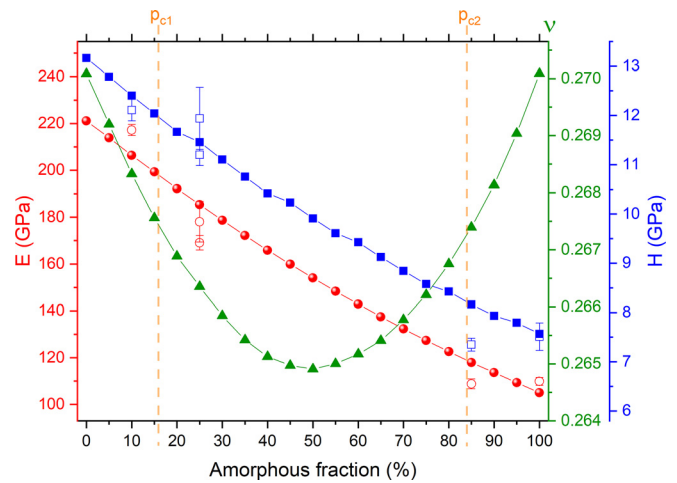


FIG. 1. Predicted mechanical properties (curves with solid symbols) in comparison with experimental data (open symbols) published in Ref. 14 as a function of amorphous fraction.

approximation, at least from mechanical point of view, as the elastic modulus and hardness of untreated crystalline Panda Hill and recrystallized initially highly damaged Miass pyrochlore (both between $\sim 20\%$ and 30% f_a after Ref. 13) appear to be comparable ($E \sim 169$ and ~ 178 GPa and $H \sim 11.2$ and 11.9 GPa, respectively) (see Ref. 14). For simplification, we assumed an average of 25% f_a for both samples in Figure 1.

Figure 2 provides details for the thermally induced structural reorganization, i.e., starting from the highly amorphized state, the establishment of percolation of the crystalline fraction (p_{c2}), and further a fully interconnected crystalline matrix, when percolation of the

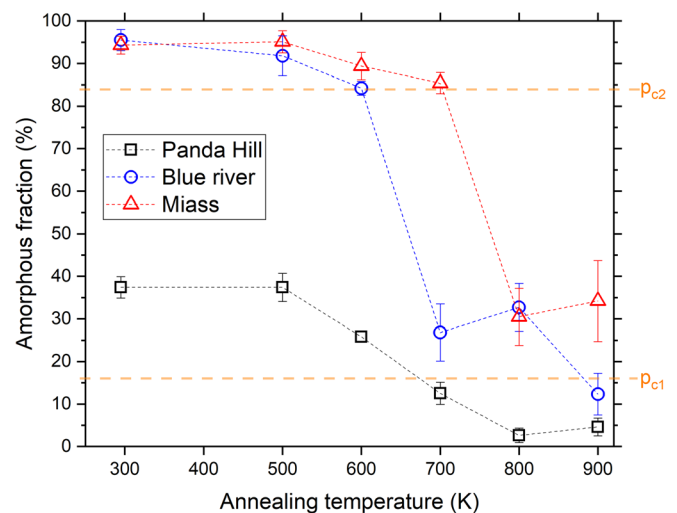


FIG. 2. Evolution of the amorphous fraction as a function of annealing temperature of pyrochlore samples Panda Hill, Blue River, and Miass. Samples were stepwise annealed for 16 h at each temperature step and subsequently cooled down to room temperature. The dashed lines are a guide for the eye.

amorphized phase ceases (p_{c1}). The modeled E_{fa} evolution from Fig. 1 has been used to determine the amorphous fractions of the pyrochlore samples (from Ref. 14) during stepwise thermal annealing (given values apply to room temperature conditions) in Fig. 2. To be more precise, the measured E values of the pyrochlore samples after each annealing experiment by Reissner *et al.*¹⁴ have been correlated with the modeled general evolution of E with increasing f_a (see Fig. 1). By mapping the changing Young's modulus along the curve in Fig. 1, the reported changes in amorphous volume fraction after stepwise annealing are determined (Fig. 2). The chosen annealing time (16 h) at each temperature step was found to be sufficient to reach saturation.¹⁴ Highly disordered Blue River (initially containing preserved crystalline areas) and Miass pyrochlore samples reach p_{c2} (84.1% f_a) after stepwise annealing at 600 and 700 K, respectively (Fig. 2). It is notable how stable the system behaves as long it stays above p_{c2} . A further increase in temperature is necessary to overcome this threshold to reach the bicontinuous structural state (between p_{c2} and p_{c1}). One can conclude that as long as both phases percolate (between both percolation thresholds) only little additional energy is needed to further increase the structural order. The initially higher crystalline Panda Hill and partially recrystallized Blue River samples exceed p_{c1} after annealing at 700 and 900 K, respectively. One can expect that Blue River pyrochlore undergoes an overall structural homogenization at least at annealing temperatures ≤ 800 K, before passing p_{c1} at higher temperatures. The formation of new phases in Miass pyrochlore at the relevant annealing temperatures (> 800 K)^{13,14} seems to prevent this step. Overcoming the first percolation point, hence establishing a crystalline matrix comprising isolated isles of amorphous areas, seems to be only possible with a certain preexisting initial amount of preserved crystalline domains.

These findings imply the need for additional energy to pass the percolation points (Fig. 2), while the required temperature depends on the initial state of crystallinity and homogeneity. Noticeable structural modifications become visible on the short- and long-range order scale after stepwise annealing at the found percolation threshold related temperatures (Fig. 2): sharpening of photoluminescence and Raman signals decreases in unit cell volume and amorphous fraction, sharpening of Bragg reflections, and an increase in elastic modulus (direct measure for the overall connectivity).^{13,14,27} As our model (Fig. 1) predicts an almost linear trend for E and H with increasing amorphization, the pronounced changes in the amorphous fraction visible in Fig. 2 can be directly attributed to changes in the mechanical properties.

In summary, mechanical modeling agrees with the direct influence of percolation transitions on the recrystallization behavior and progress in radiation damaged pyrochlore. Both percolation thresholds can be assumed to act as specific kinetic barriers during thermally induced structural reorganization, strongly depending on the initial degree of structural order. After exceeding the percolation points, changes in short- and long-range order are noticeable in literature data.^{13,14,27} This is an important point that has to be considered for estimating a materials' potential as a nuclear waste matrix or to be used in high radiation environments, e.g., for space applications. This study further validates the efficiency and robustness of the used model to approximate the mechanical behavior of, at least, ceramic materials during the crystalline-to-amorphous transition. The approach could be helpful for generating additional data for training neural networks,

as Ref. 28 already mentioned that simulated data can be a useful addition to complete datasets.

This research was funded by the Deutsche Forschungsgemeinschaft (DFG, German Research Foundation)—No. BE 5456/2-1 (T.B.).

AUTHOR DECLARATIONS

Conflict of Interest

The authors have no conflicts to disclose.

DATA AVAILABILITY

The data that support the findings of this study are available from the corresponding authors upon reasonable request.

REFERENCES

- Y. Yasui, M. Soda, S. Iikubo, M. Ito, M. Sato, N. Hamaguchi, T. Matsushita, N. Wada, T. Takeuchi, N. Aso, and K. Kakurai, *J. Phys. Soc. Jpn.* **72**, 3014 (2003).
- R. C. Ewing, W. J. Weber, and J. Lian, *J. Appl. Phys.* **95**, 5949 (2004).
- J. Cheng, J. Li, C. Ma, and Z. Hao, *Catal. Commun.* **10**, 1170 (2009).
- K. Matsushita, M. Tokunaga, M. Wakeshima, Y. Hinatsu, and S. Takagi, *J. Phys. Soc. Jpn.* **82**, 023706 (2013).
- E. Öztürk and E. Sarıalmaz, *Mater. Res. Express* **6**, 105710 (2019).
- R. C. Ewing, *Proc. Natl. Acad. Sci. U. S. A.* **96**, 3432 (1999).
- G. R. Lumpkin, Y. Gao, R. Gieré, C. T. Williams, A. Mariano, and T. Geisler, *Miner. Mag.* **78**, 1071 (2014).
- B. C. Chakoumakos, *J. Solid State Chem.* **53**, 120 (1984).
- G. R. Lumpkin, *J. Nucl. Mater.* **289**, 136 (2001).
- G. R. Lumpkin and R. C. Ewing, *Phys. Chem. Miner.* **16**, 2 (1988).
- R. C. Ewing, A. Meldrum, L. M. Wang, and S. X. Wang, *Rev. Miner. Geochem.* **39**, 319 (2000).
- G. R. Lumpkin, E. M. Foltyn, and R. C. Ewing, *J. Nucl. Mater.* **139**, 113 (1986).
- P. Zietlow, T. Beirau, B. Mihailova, L. A. Groat, T. Chudy, A. Shelyug, A. Navrotsky, R. C. Ewing, J. Schlüter, R. Škoda, and U. Bismayer, *Z. Kristallogr.* **232**, 25 (2017).
- C. E. Reissner, V. Roddatis, U. Bismayer, A. Schreiber, H. Pöhlmann, and T. Beirau, *Materialia* **14**, 100950 (2020).
- M. Zhang and E. K. H. Salje, *Phase Transitions* **76**, 117 (2003).
- T. Beirau, A. Shelyug, A. Navrotsky, H. Pöhlmann, and E. K. H. Salje, *Appl. Phys. Lett.* **115**, 231904 (2019).
- E. K. H. Salje, J. Chrosch, and R. C. Ewing, *Am. Miner.* **84**, 1107 (1999).
- G. R. Lumpkin, "Ceramic host phases for nuclear waste remediation," in *Experimental and Theoretical Approaches to Actinide Chemistry*, edited by J. K. Gibson and W. A. de Jong (Wiley, 2018), p. 333.
- C. Soyarslan, S. Bargmann, M. Pradas, and J. Weissmüller, *Acta Mater.* **149**, 326 (2018).
- N. Huber and T. Beirau, *Scr. Mater.* **197**, 113789 (2021).
- J. W. Cahn, *J. Chem. Phys.* **42**, 93 (1965).
- A. P. Roberts and E. J. Garboczi, *J. Mech. Phys. Solids* **47**, 2029 (1999).
- M. Zhao, X. Ren, W. Pan, and J. Europ, *Ceram. Soc.* **35**, 1055 (2015).
- J. Feng, B. Xiao, Z. X. Qu, R. Zhou, and W. Pan, *Appl. Phys. Lett.* **99**, 201909 (2011).
- F. W. Clinard, Jr., D. E. Peterson, D. L. Rohr, and L. W. Hobbs, *J. Nucl. Mater.* **126**, 245 (1984).
- G. R. Lumpkin and T. Geisler-Wierwille, "Minerals and natural analogues," in *Comprehensive Nuclear Materials*, edited by R. J. M. Konings (Elsevier, 2012), Chap. 5.22, Vol. 5, pp. 563–600.
- P. Zietlow, "Properties and recrystallization of radiation damaged pyrochlore and titanite," PhD dissertation (University of Hamburg, Germany, 2016).
- L. Lu, M. Dao, P. Kumar, U. Ramamurty, G. E. Karniadakis, and S. Suresh, *Proc. Natl. Acad. Sci. U. S. A.* **117**, 7052 (2020).